

**Glycobiology and Extracellular Matrices:
Biosynthesis of UDP-4-keto-6-deoxyglucose
and UDP-rhamnose in Pathogenic Fungi
Magnaporthe grisea and *Botryotinia
fuckeliana***



Viviana Martinez, Miles Ingwers, James
Smith, John Glushka, Ting Yang and Maor
Bar-Peled

J. Biol. Chem. 2012, 287:879-892.

doi: 10.1074/jbc.M111.287367 originally published online November 18, 2011

Access the most updated version of this article at doi: [10.1074/jbc.M111.287367](https://doi.org/10.1074/jbc.M111.287367)

Find articles, minireviews, Reflections and Classics on similar topics on the [JBC Affinity Sites](#).

Alerts:

- [When this article is cited](#)
- [When a correction for this article is posted](#)

[Click here](#) to choose from all of JBC's e-mail alerts

Supplemental material:

<http://www.jbc.org/content/suppl/2011/11/18/M111.287367.DC1.html>

This article cites 35 references, 12 of which can be accessed free at
<http://www.jbc.org/content/287/2/879.full.html#ref-list-1>

Biosynthesis of UDP-4-keto-6-deoxyglucose and UDP-rhamnose in Pathogenic Fungi *Magnaporthe grisea* and *Botryotinia fuckeliana**^[5]

Received for publication, July 28, 2011, and in revised form, October 25, 2011. Published, JBC Papers in Press, November 18, 2011, DOI 10.1074/jbc.M111.287367

Viviana Martinez[‡], Miles Ingwers[§], James Smith[‡], John Glushka[‡], Ting Yang[¶], and Maor Bar-Peled^{‡§1}

From the [‡]Complex Carbohydrate Research Center and Departments of [§]Plant Biology and [¶]Biochemistry and Molecular Biology, University of Georgia, Athens, Georgia 30602

Background: Rhamnose-containing glycans are involved in host-pathogen interactions.

Results: UDP-rhamnose was identified in fungi; recombinant enzymes involved in its synthesis were characterized, and the genes involved are expressed in a tissue-specific manner.

Conclusion: Fungi containing rhamnose likely utilize the UDP-rhamnose pathway.

Significance: Understanding rhamnose pathways in fungi may provide new insight to fungus-host interaction.

There is increasing evidence that in several fungi, rhamnose-containing glycans are involved in processes that affect host-pathogen interactions, including adhesion, recognition, virulence, and biofilm formation. Nevertheless, little is known about the pathways for the synthesis of these glycans. We show that rhamnose is present in glycans isolated from the rice pathogen *Magnaporthe grisea* and from the plant pathogen *Botryotinia fuckeliana*. We also provide evidence that these fungi produce UDP-rhamnose. This is in contrast to bacteria where dTDP-rhamnose is the activated form of this sugar. In bacteria, formation of dTDP-rhamnose requires three enzymes. Here, we demonstrate that in fungi only two genes are required for UDP-Rha synthesis. The first gene encodes a UDP-glucose-4,6-dehydratase that converts UDP-glucose to UDP-4-keto-6-deoxyglucose. The product was shown by time-resolved ¹H NMR spectroscopy to exist in solution predominantly as a hydrated form along with minor amounts of a keto form. The second gene encodes a bifunctional UDP-4-keto-6-deoxyglucose-3,5-epimerase/-4-reductase that converts UDP-4-keto-6-deoxyglucose to UDP-rhamnose. Sugar composition analysis and gene expression studies at different stages of growth indicate that the synthesis of rhamnose-containing glycans is under tissue-specific regulation. Together, our results provide new insight into the formation of rhamnose-containing glycans during the fungal life cycle. The role of these glycans in the interactions between fungal pathogens and their hosts is discussed. Knowledge of the metabolic pathways involved in the formation of rhamnose-containing glycans may facilitate the development of drugs to combat fungal diseases in

humans, as to the best of our knowledge mammals do not make these types of glycans.

Necrotrophic and biotrophic fungal pathogens are a major cause of global crop damage. Necrotrophic fungi, including *Botryotinia fuckeliana* (*Botrytis cinerea*), attach to the host and then secrete enzymes and toxins that kill host cells prior to pathogen invasion (1). In contrast, biotrophic pathogens, including *Magnaporthe grisea* (*Magnaporthe oryzae*), proliferate within living plant tissues and cause tissue damage and yield reduction. *M. grisea*, which causes rice blast disease (2), is a major threat to the food supply. It is estimated that *M. grisea* destroys enough rice to feed 60 million people in a given year (3). Likewise *B. fuckeliana* has an agricultural and economic impact on over 200 plant species (4).

There is increasing evidence that changes in the glycans present on the fungal cell surface play a role during the infection process (5, 6). For example, the ability of a fungus to infect its host is reduced by biochemical treatments that impair glycan recognition or remove the glycan moiety (7). Here, we discuss the potential role of the surface residue rhamnose in fungi.

Rhamnose (Rha, 6-deoxy-L-mannose) has been reported to be present in a variety of glycoproteins, exopolysaccharides (EPS),² and some minor components of the fungal cell wall. For example, hyphae from the barley pathogen *Rhynchosporium secalis* contain rhamnomannans (8) that are tightly associated with the cell walls. Other types of rhamnomannans are solubilized by alkali. Rhamnose accounts for at least 30% of the sugars in the rhamnomannan of *Cephalotheca purpurea* and *Cephalotheca reniformis* (9) and less than 2% in *Penicillium chrysogenum* and *Ophiostoma ulmi* (10, 11).

In addition, *Cryphonectria parasitica*, the causal agent of chestnut blight disease, secretes an EPS composed of a mannan

* This work was supported in part by National Science Foundation Grant IOB-0453664 (to M. B.-P.) and by BioEnergy Science Center Grant DE-PS02-06ER64304 (supported by the Office of Biological and Environmental Research in the Department of Energy Office of Science).

^[5] This article contains supplemental Figs. S1 and S2, Tables S1–S7, and additional references.

The nucleotide sequence(s) reported in this paper has been submitted to the GenBank™/EBI Data Bank with accession number(s) JF740056, JF740057, JF740058, and JF740059.

¹ To whom correspondence should be addressed: Complex Carbohydrate Research Center, 315 Riverbend Rd., Athens, GA 30602. Tel.: 706-542-2062; Fax: 706-542-4412; E-mail: peled@crcr.uga.edu.

² The abbreviations used are: EPS, exopolysaccharide; HSQC, heteronuclear single quantum coherence; HMBC, heteronuclear molecular bond coherence; UG4,6-DH, UDP-Glc 4,6-dehydratase; U4k6dG-ER, UDP-4-keto-6-deoxyglucose-3,5-epimerase/-4-reductase; U4k6dG, UDP-4-keto-6-deoxyglucose; NRS/ER, nucleotide-rhamnose synthase/epimerase-reductase.

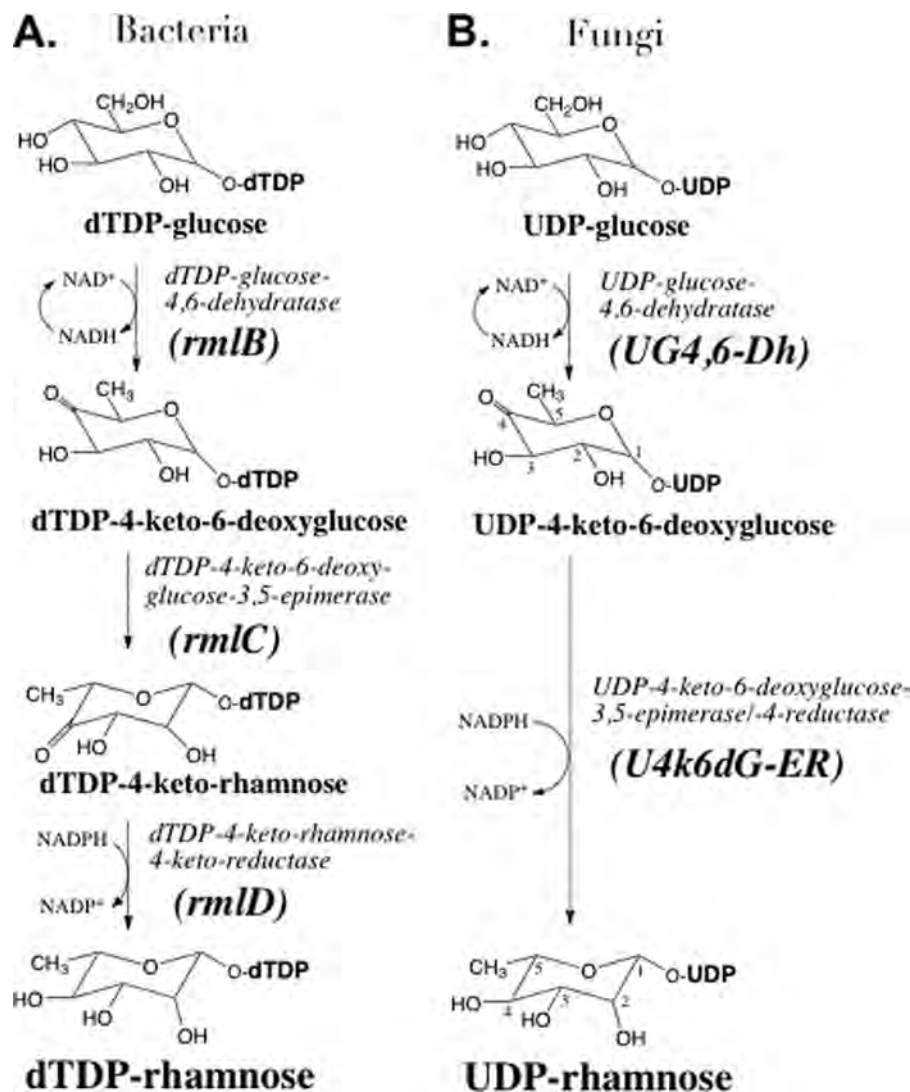


FIGURE 1. **Biosyntheses of NDP-4-keto-6-deoxyglucose and NDP-rhamnose in fungi, plants, and bacteria.** *A*, in bacteria, *Streptococcus suis*, dTDP-Glc pyrophosphorylase (*rmlA*) converts Glc-1-P and dTTP to dTDP-Glc (38). dTDP-Glc is interconverted by *rmlB*, dTDP-4-keto-6-deoxyglucose dehydratase (via two theoretical intermediates, dTDP-4-keto-glucose and dTDP-4-keto-6-deoxyglucose-5,6-ene), into dTDP-4-keto-6-deoxyglucose (*U4k6dG*) and H₂O (25). *rmlC*, a 3,5-epimerase, converts dTDP-4k6dG to dTDP-4-keto-rhamnose that is 4-reduced by *rmlD* in the presence of NADPH to dTDP-Rha and NADP⁺. *B*, in fungi (this study) UDP-Glc is interconverted by 4,6-dehydratase (*UG4,6-Dh*) into UDP-4-keto-6-deoxyglucose (*U4k6dG*) and H₂O. A bi-functional 3,5-epimerase and 4-reductase (*U4k6dG-ER*) converts *U4k6dG* to UDP-Rha and NADP⁺. In plants (18, 19) one enzyme has 4,6-dehydratase, 3,5-epimerase, and 4-reductase activities to convert UDP-Glc to UDP-Rha.

backbone that is decorated with oligosaccharide side chains that are terminated with rhamnose (12). Interestingly, nonvirulent strains of this fungus do not secrete this EPS. The mucilage secreted by fungal spores of the corn pathogen, *Colletotrichum graminicola* consists of various glycoproteins containing Rha as well as galactose and mannose residues (13). These glycoproteins have been proposed to function as an antidesiccant thereby allowing *Colletotrichum* conidia to survive periods of drought and changes in temperature (6).

Although the biosynthesis of fungal core wall polysaccharides (e.g. glucan, chitin, and mannan) is relatively well understood, virtually nothing is known about the biosynthesis of Rha-containing glycans in fungi, nor is the identity of the activated form of rhamnose used in the synthesis of these glycans known.

Numerous studies have established that dTDP-rhamnose (dTDP-Rha) is used by bacteria for the synthesis of Rha-containing glycolipids and polysaccharides (14). This nucleotide

sugar is formed from dTDP-glucose (dTDP-Glc) (Fig. 1A) by three different enzymes. A 4,6-dehydratase (*rmlB*) converts dTDP-Glc to dTDP-4-keto-6-deoxyglucose. This product is then converted to dTDP-4-keto-rhamnose by a 3,5-epimerase (*rmlC*). An enzyme with 4-reductase activity (*rmlD*) converts the keto-rhamnose to dTDP-Rha (15–17). Plants have a single protein (Rhm (UDP-L-rhamnose synthase) also annotated as URS) that converts UDP-Glc to UDP-Rha (18, 19). In addition, plants have a bi-functional protein (nucleotide-rhamnose synthase/epimerase-reductase (NRS/ER)) that has 3,5-epimerization and 4-reduction activities (19).

Here, we describe the identification and functional characterization of two genes from *M. grisea* and *B. fuckeliana* involved in UDP-Rha formation. One gene encodes a 4,6-dehydratase, and the second encodes a bifunctional enzyme with 3,5-epimerase and 4-reductase activities (Fig. 1B). Such enzyme activities have not previously been described in fungi, and thus

our data provide a basis for understanding the formation of fungal Rha-containing glycans and their roles during the various life cycles of these pathogens.

EXPERIMENTAL PROCEDURES

Fungal Strains—*M. grisea* (Hebert) Barr strain CP987 and *B. cinerea* strain B05.10 (*B. fuckeliana*) were obtained from Dr. S.-C. Wu and Dr. C. Bergman, respectively, of the Complex Carbohydrate Research Center.

Cloning of UG4,6-Dh and U4k6dG-ER from Fungi—TRIzol reagent (Invitrogen) was used to isolate total RNA from a 14-day-old sporulated culture of *M. grisea* grown at 24 °C on oatmeal agar (20) and from 2-week-old *B. fuckeliana* grown at 24 °C on potato dextrose agar. RNA was reverse-transcribed with oligo(dT) as a primer using RT-superscript III (Invitrogen). The cDNAs were used as templates in PCR to amplify the coding sequences of MGG_06324 and BC1G_06494 (herein named UDP-Glc 4,6-dehydratase and abbreviated as UG4,6-Dh) and MGG_09238, BC1G_01271 (herein named UDP-4-keto-6-deoxyglucose-3,5-epimerase/-4-reductase and abbreviated as U4k6dG-ER) using Platinum DNA polymerase (Invitrogen) or PHUSION polymerase (New England Biolabs). The forward and reverse PCR primers are listed in [supplemental Table S1](#). Each PCR product was separated and isolated from Tris/acetate/EDTA (TAE)-agarose and TOPO TA-cloned to generate plasmids pCR4:MgDh, pCR4:MgER, pCR4:BfDh, and pCR4:BfER, respectively. Following DNA sequence analyses and subsequent biochemical characterization, the genes were annotated as Mg-UG4,6-Dh, Bf-UG4,6-Dh, Mg-U4k6dG-ER, and Bf-U4k6dG-ER, and their sequences were deposited in GenBank™ (MgDh, accession number JF740056; MgER, accession number JF740057; BfDh, accession number JF740058; BfER, accession number JF740059). The PciI-NotI fragment (1296bp-Mg; 1300bp-Bf) containing the UG4,6-Dh coding sequence and the PciI-NotI fragment (882bp-Mg; 897bp-Bf) of U4k6dG-ER, each without a stop codon, were cloned into the NcoI/NotI sites of an *Escherichia coli* expression vector (pET28b-Tev (21)). This generates a recombinant protein with a dual six-histidine extension at the N and C termini. Alternatively Mg-UG4,6-Dh and Mg-U4k6dG-ER were amplified by PCR from cDNA using primers with 15-nucleotide perfect homology to linearize NcoI/NotI-digested pET28-Tev 1.15 vector and cloned directly by a proprietary in-fusion reaction (Novagen).

Expression and Purification of Recombinant UG4,6-Dh and U4k6dG-ER—BL21-derived *E. coli* cells containing the *M. grisea* and *B. fuckeliana* recombinant UG4,6-Dh and U4k6dG-ER in pET28bTev plasmids or a control empty vector (pET28b) were cultured for 16 h at 37 °C in LB medium (20 ml) supplemented with kanamycin (50 µg/ml) and chloramphenicol (35 µg/ml). A portion (5 ml) of the cultured cells was transferred into fresh LB liquid medium (250 ml) supplemented with the same antibiotics and then grown at 37 °C at 250 rpm until the culture had an A_{600} of 0.8. Gene expression was then induced by the addition of isopropyl β -D-thiogalactoside (0.5 mM), and the cells were then grown for 20 h at 18 °C at 250 rpm. Cells were harvested by centrifugation (6,000 \times g for 10 min at 4 °C) and suspended in lysis buffer (10 ml). For UG4,6-Dh, 50 mM Tris-

HCl, pH 7.5, containing 150 mM NaCl, 10% glycerol, and 1 mM EDTA was used. The same buffer, pH 9, supplemented with 2 mM DTT and 0.5 mM phenylmethylsulfonyl fluoride was used for U4k6dG-ER. Cells were lysed in an ice bath with a Misonix S-4000 sonicator (Misonix Inc, Farmingdale, NY) equipped with 1/8-inch microtip probe using 12 sonication cycles each (20-s pulse; 30 s off). The lysed cells were centrifuged (6,000 \times g for 10 min at 4 °C); the supernatant was supplemented with 1 mM DTT and centrifuged again (20,000 \times g for 30 min at 4 °C). The resulting supernatant (termed S20) was kept at -20 °C. His-tagged proteins were purified on a fast-flow nickel-Sepharose (GE Healthcare, 2 ml of resin packed in a 1-cm inner diameter \times 15-cm polypropylene column). For UG4,6-Dh, the column was pre-equilibrated with loading buffer 50 mM sodium phosphate, pH 8 (pH 9 for U4k6dG-ER), containing 0.3 M NaCl and 1 mM DTT. The bound His-tagged protein was eluted with the same buffer containing increased concentrations of imidazole (10–250 mM). The fraction containing the enzymatic activity, typically eluted with 250 mM imidazole, was dialyzed (6,000–8,000 molecular weight cutoff, Spectrum Laboratories, Inc.) at 4 °C three times against 50 mM Tris-HCl, pH 8 (pH 9 for U4k6dG-ER), containing 0.15 M NaCl, 10% glycerol, 1 mM DTT, 10 µM NAD⁺ for 2 h. The dialysate was divided into 0.25-ml aliquots that were flash-frozen in liquid nitrogen and kept at -80 °C.

Proteins extracted from *E. coli* cells expressing the empty vector were obtained using the same purification protocol and were used as controls in enzyme assays and SDS-PAGE analyses. Protein concentrations were determined using the Bradford reagent with bovine serum albumin (BSA) as standard. The native molecular weight of each recombinant protein was estimated by Superdex 75 size-exclusion chromatography as described (22) using dialysis buffer as eluant.

UG4,6-Dh and U4k6dG-ER Enzyme Assays—UG4,6-Dh reactions (50-µl final volume) were carried out in 50 mM sodium phosphate, pH 7.6, containing 1 mM NAD⁺, 2 mM UDP-Glc, and 13 µg of purified recombinant UG4,6-Dh. U4k6dG-ER reactions (60-µl final volume) were carried out in 50 mM sodium phosphate, pH 7.6, containing 3 mM NADPH, 1 mM NAD⁺, 2 mM UDP-Glc, purified recombinant UG4,6-Dh, and purified recombinant U4k6dG-ER (17 µg). Reactions were kept for up to 45 min at 30 °C and then terminated (100 °C water bath, 1 min). Chloroform (50 µl) was added; the mixture was vortexed and centrifuged (12,000 rpm, 5 min at 22 °C). The upper aqueous phase was collected. Reaction products were chromatographed on an anion-exchange column (Q15 resin in 1-mm inner diameter \times 250 mm, Amersham Biosciences; or Mono Q 5 \times 50 mm, Amersham Biosciences) eluted with a linear gradient of ammonium formate (5 mM to 0.6 M) (22) over 25 min, using an Agilent 1200 Series HPLC system equipped with an autosampler, diode array detector, and ChemStation software. Nucleotides were detected by their A_{261} (maximum for UDP-sugar) and A_{259} (maximum for NAD⁺). The amount of product formed was determined using a calibration curve of standard UDP-Glc. The products formed by the UG4,6-Dh reaction (eluted at 12.3 min from Q-column) and the U4k6dG-ER reaction (eluted at 13.2 min from the PA1 column)

UDP-rhamnose Formation in Fungi

were collected, lyophilized, dissolved in water or 99.9% D₂O, and analyzed by ESI-MS and by ¹H NMR spectroscopy.

Characterization of Recombinant Enzymes—UG4,6-Dh activities were determined using different buffers, different temperatures, and in the presence of selected cations or potential inhibitors. For pH studies, solutions of recombinant UG4,6-Dh (13 μg) were mixed in each individual buffer (50 mM). Subsequently, NAD⁺ (1 mM) and UDP-Glc (2 mM) were added, and reactions were carried out for 30 min at 30 °C. Inhibition assays were performed by first mixing the enzyme and buffer with different additives (e.g. nucleotides) on ice for 10 min. UDP-Glc and NAD⁺ (1 mM each) were then added. After 30 min at 30 °C, the amount of UDP-sugar formed was determined by ¹H NMR spectroscopy.

Real Time ¹H NMR-based Enzyme Assay—Real time ¹H NMR spectroscopic monitoring of enzymatic reactions (150 μl) was performed at 30 °C in a mixture of D₂O/H₂O (9:1 v/v), containing 50 mM sodium phosphate at various pH values, and 1–1.5 mM UDP-Glc, 0.6 mM NAD⁺, and 13 μg of recombinant UG4,6-Dh. The combined UG4,6-Dh and U4k6dG-ER NMR assay used the same buffer supplemented with 1.5 mM NADPH. Real time ¹H NMR spectra were obtained using a Varian VNMRS spectrometer operating at 600 MHz and equipped with a 3-mm cold probe. Data acquisition was started between 2 and 5 min after the addition of enzyme to allow spectrometer acquisition conditions to be optimized. Sequential one-dimensional proton spectra with presaturation of the water resonance were acquired over the course of the enzymatic reaction, with spectra summed and averaged every 8 s. All chemical shifts (ppm) are referenced to 2,2-dimethyl-2-silapentane-5-sulfonate (δ0.00). ¹³C-Enriched UDP-4-keto-6-deoxyglucose was prepared from UDP-[¹³C]Glc using recombinant Sloppy (UDP-sugar pyrophosphorylase (USP)) (21), UTP, and [¹³C]Glc-1-P (OMICRON Biochemicals, Inc.). Subsequently, the 4,6-dehydratase with or without the U4k6dG-ER was added. The reaction mixtures, which contained UDP-[¹³C]Glc, UDP-[¹³C]4k6dG, and UDP-[¹³C]Rha, were examined by ¹³C HSQC and ¹³C HMBC NMR experiments using standard Varian pulse programs.

Isolation and Glycosyl Residue Analyses of Fungal Polysaccharides—Freeze-dried spores of fungal strains, stored in –80 °C on filter paper, were grown on Potato Dextrose Broth (*B. fuckeliana*) or oatmeal agar plates (*M. grisea*) for 10–14 days at 22 °C; conidia were washed off the agar with 10 ml of sterile water, and the suspension was filtered through eight layers of cheesecloth. The filtered suspension was allowed to settle, and the water above the spores was removed. The spores were resuspended in sterile water and diluted to 2 × 10⁵ spores per ml and used to inoculate 500 ml of Potato Dextrose Broth or CM-Suc (*B. fuckeliana*), Vogel-Suc, or CM-Suc (*M. grisea*) media. After 7 days of growth at 25 °C with shaking (150 rpm) or without shaking, hyphae were collected on Miracloth, and the filtrate (cultured media) was saved. The hyphae ball was washed with water and freeze-dried, and the hyphal powder was weighed. The filtered culture media were concentrated to 100 ml by rotary evaporation and then 2 volumes of ethanol were added to precipitate EPS. The suspension was centrifuged

(8,000 × g for 15 min, 4 °C), and the pellet was washed with aqueous 95% ethanol, dried, and resuspended in water.

Two extraction methods were used to isolate glycans from the hyphal powder. In the first procedure, the hyphal powder (1 g) was treated sequentially (twice each time) with 8 ml of EtOH (80%), 5 ml of chloroform/MeOH (1:1 v/v), and 4 ml of acetone. The sugar composition of the resulting residue (termed AIR) as well as of each derived organic extract (termed Et, CM, and Ac) was dried by a stream of air and determined. In the second procedure, the hyphal powder (5 g) was treated for 4 h at 22 °C while stirring with 1 M NaOH (200 ml) three times. After centrifugation (10,000 × g, 4 °C, 10 min) the combined alkaline extracts were mixed with an equal volume of 96% ethanol. The pellet that formed was collected by centrifugation (10,000 × g, 4 °C, 15 min), resuspended in water (10 ml), and dialyzed (3,000 molecular weight cutoff) against two 10-liter changes of deionized water. The dialyzed solution was clarified by centrifugation (10,000 × g, 4 °C, 15 min) and the water-soluble supernatant (aWS) was collected and freeze-dried (yield ~250 mg). The residue remaining after centrifugation (termed aWi) was washed with water, dried, and weighed (~150 mg). The glycosyl residue compositions of these extracts were then determined.

Glycosyl Residue Composition Analysis—Each extract (1 mg) was hydrolyzed for 2 h at 120 °C with 2 M TFA (1 ml). The TFA was removed by evaporation under a stream of filtered air (40 °C) followed by three cycles of wash with isopropyl alcohol (500 μl) and solvent evaporation. The resulting dried neutral monosaccharides were converted into their corresponding alditols in 500 μl of reducing solution (10 mg/ml sodium borodeuteride in 1 M NH₄OH) for 1 h at 22 °C. The reaction was quenched with glacial acetic acid (500 μl), and the solution was concentrated to dryness. The residue was washed three times with MeOH/OHAc 9:1 v/v (1 ml) and then with MeOH (three times, 1 ml). The alditols were converted to their corresponding alditol-acetate derivatives (23) by treatment for 20 min at 120 °C with acetic anhydride (150 μl) and pyridine (100 μl). The reagents were removed under a stream of air, and the residue was washed with hexane (three times, 1 ml), and then water (1 ml) was added. After sample sonication, the alditol acetates were extracted into dichloromethane (1 ml). The organic phase was concentrated to dryness, and the residue was dissolved in acetone (100 μl). Samples were analyzed by gas-liquid chromatography (GLC) equipped with a flame ionization detector or with a mass selective detector (EI-MS). The sample (1 μl) was injected in the split mode (1:50 split) using an Agilent 7890A autosampler to a Restek RTx-2330 (or SP-2330, Supelco) fused silica column (0.25 mm inner diameter × 30 m, 0.2-μm film thickness) with helium as gas carrier at a flow rate of 1.1 ml min⁻¹. The GC program was started with the oven temperature held at 80 °C for 2 min, followed by an increase of 30 °C min⁻¹ to 170 °C, then at 4 °C min⁻¹ to 235 °C, and a hold at 235 °C for 20 min. The column was then kept at 250 °C for 7 min cooled to 80 °C and kept at 80 °C for 1 min prior to the next sample injection. The injection port and the flame ionization detector were kept at 250 °C. GC-MS was performed with an HP 5973 MSD. Alditol-acetate derivatives of monosaccharide standards (50 μg each of rhamnose, fucose, ribose, arabinose, xylose, mannose, glucose, and galactose) were prepared under the same condi-

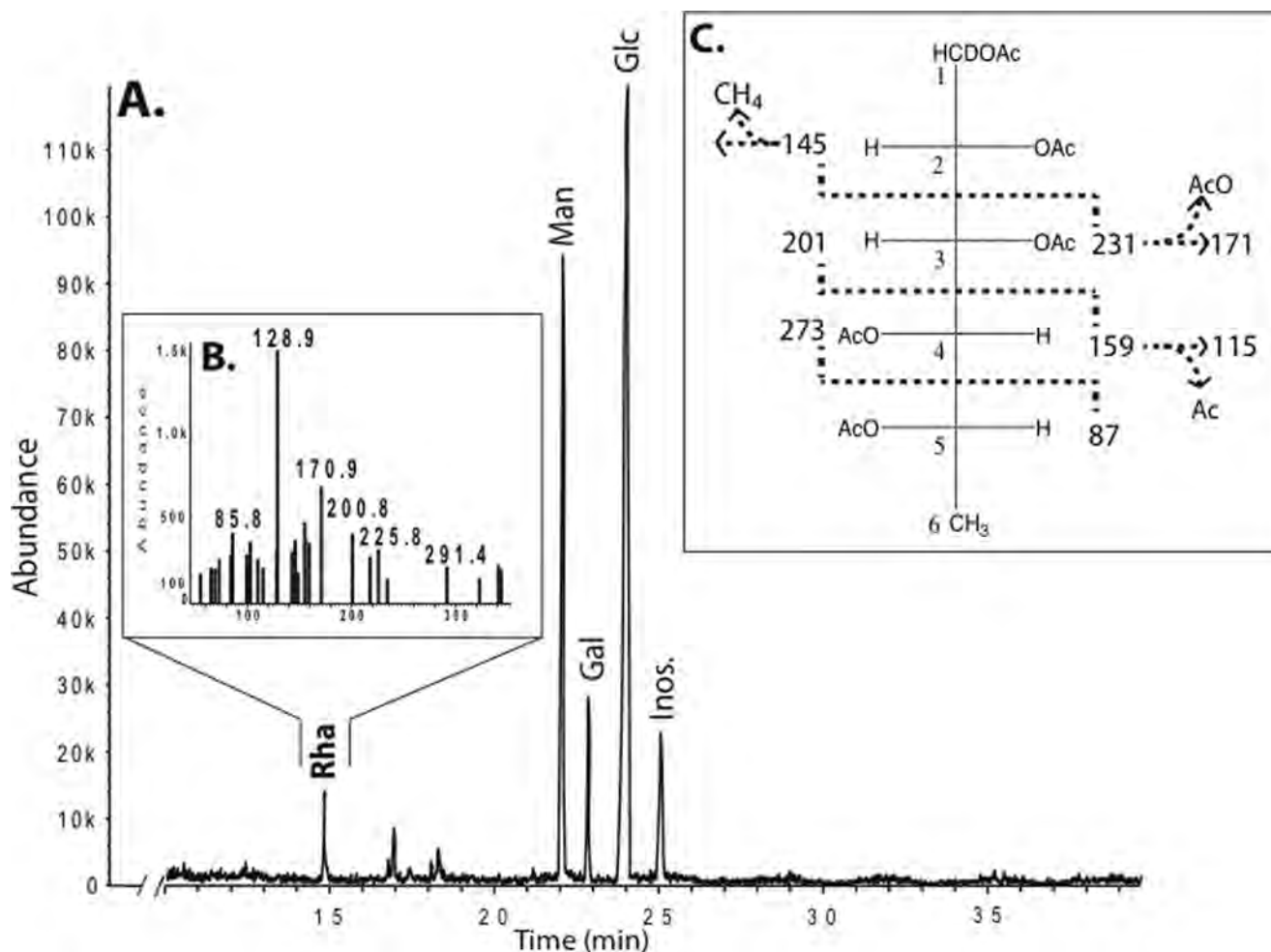


FIGURE 2. **Glycosyl residue compositions of rhamnose-containing glycans *B. fuckeliana*.** A, GC spectrum of alditol-acetates derived from EPS of *B. fuckeliana* grown for 10 days in CM liquid media under continuous shaking. The peak eluting at 14.85 min has the same retention time as authentic rhamnose standard, and EI-MS fragmentation pattern of the sample peak (see B, inset) showed the same fragmentation pattern as standard rhamnose. The annotated sugar peaks of the spectrum are based on elution of standard and EI-MS fragmentation: rhamnose (*Rha*), mannose (*Man*), galactose (*Gal*), and glucose (*Glc*); the peaks labeled * were not identified. Inositol (*Ino*) is the internal control. C, right inset shows theoretical fragmentation of ionized rhamnitol-acetate derivative. Note the diagnostic ion at m/e 171 is derived from the acetate anion loss from 231.

tions as samples. Myoinositol (20 μ g) was added as internal standard. For data analysis, sugar residue peaks were identified based on retention times of standard monosaccharides and their characteristic mass spectrum. The raw peak areas, obtained from the total ion chromatogram, were exported to Microsoft Excel and normalized to sample mass and the internal standard. The amount of individual residue in samples was calculated based on calibration curves of standards.

Nucleotide Sugar Extraction and Analyses—Fungal tissues (hyphae grown in 100 ml of CM media for 7 days at 25 °C; spores from CM-agar) were collected on a filter, washed with water, and weighed. Cold 0.2 M sodium fluoride (1 ml) was added per 0.5 g wet weight cells. The suspension was vortexed for 1 min, then 6 volumes of cold chloroform/MeOH (1:1 v/v) was added, and the mixture was kept for 30 min at 4 °C during which the sample was vortexed for 20 s every 3 min. The suspension was centrifuged (1,000 \times g for 4 min), and the aqueous layer was transferred to a new tube and centrifuged again to remove debris. Portions (30 μ l) were injected via HPLC at 0.25 ml min⁻¹ to a Q15 column (1 mm inner diameter \times 250 mm) pre-equilibrated with 20 mM ammonium formate, and separa-

tion was achieved over a 25-min gradient by increasing the concentration of ammonium formate (22). Column fractions (0.4 ml) were collected, and a portion (350 μ l) was lyophilized and then dissolved in D₂O (150 μ l) for ¹H NMR analysis. The remaining material was analyzed by ESI-MS/MS.

ESI-MS/MS—ESI-MS/MS was performed with an LTQ-XL or LCQ-Advantage (ThermoFisher) mass spectrometer operating in the negative ion mode (de-protonated [M-H]⁻). An aliquot (47.5 μ l) of each column fraction or standard nucleotide-sugar (0.1–100 μ M) was mixed with 2.5 μ l of 0.4 M triethylammonium acetate, pH 7, and 50 μ l of acetonitrile. Sample (5–20 μ l) was delivered via the HPLC autosampler (Surveyor, 200 μ l loop) into the ion source at 25 μ l min⁻¹ with solvent A: 9 mM triethylammonium acetate, pH 7 in 50% acetonitrile (24). Negative ion mass spectra were recorded over the range of 150–2,000 m/z for 10 min. MS-MS experiments were performed by collision-induced dissociation (collision voltages 20, 25, 28%; collision gas helium at 40 p.s.i.).

Expression of UDP-Rha Biosynthetic Genes—TRIzol reagent (Invitrogen) was used to isolate total RNA from a 14-day-old sporulated culture of *M. grisea* grown at 24 °C on oatmeal agar

UDP-rhamnose Formation in Fungi

(20), from 10-day-old mycelium grown on CM (20), and from 14-day-old spores of *B. fuckeliana* grown at 24 °C on potato dextrose agar, and mycelium grown in PD broth. RNA (0.5 μg) was reverse-transcribed with oligo(dT) as a primer using RT-superscript III (Invitrogen). The cDNAs were used to amplify the coding sequences of corresponding UDP-Rha biosynthetic genes using Taq-DNA polymerase (Promega), and primers are listed in [supplemental Table S1](#). For transcript control, primers to amplify *Ces1* and *Arg2* (20) were used.

RESULTS

Identification of Rhamnose-containing Glycans from *M. grisea* and *B. fuckeliana*—To determine whether *M. grisea* and *B. fuckeliana* produce glycans that contain rhamnosyl residue, the glycosyl residue compositions of different fungal structures were analyzed. The alcohol insoluble wall (AIR) fraction of *M. grisea* spores obtained from fungus grown on CM agar contained mannose, galactose, and a peak (RT 14.85 min) that eluted like standard rhamnose ([supplemental Fig. S1A](#)). This peak and the Rha standard had identical EI-MS fragmentation patterns ([supplemental Fig. S1B](#)) with a diagnostic ion at m/e 171. A peak corresponding to Rha was also detected in the EPS of *B. fuckeliana* (Fig. 2A) and in the alkaline-extracted water soluble fraction from the hyphae of *B. fuckeliana*.

We next determined if *M. grisea* and *B. fuckeliana* produced an activated form of Rha. To this end, buffer extracts of *M. grisea* hyphae and spores were analyzed for the presence of nucleotide-sugars by LC-MS/MS. A peak corresponding to UDP-Rha ($[M - H]^-$ at m/z 549.76) was identified in *M. grisea* spores (see [supplemental Fig. S2B](#)). Collision-induced fragmentation of the parent ion (m/z 549.76) gave an ion at m/z 323.69 corresponding to UMP. Interestingly, the relative abundance of the UDP-Rha ion was higher than UDP-Glc in spores. To determine the genes involved in the synthesis of the rhamnose-linked glycans, we decided to first identify those that may be involved in the formation of the activated rhamnose, as these were not previously described to exist in fungi.

Identification, Cloning, and Biochemical Characterization of Fungal UG4,6-Dh—To identify fungal genes involved in the formation of activated rhamnose, we performed BLAST searches using amino acid sequences from bacterial and plant proteins known to be involved in this process. BLAST searches using bacterial rmlB (ADR74235 and BAS1138) and plant NDP-Rha synthase (At1g53500, URS) identified potential homologs in *M. grisea* and *B. fuckeliana*. The *M. grisea* homolog shares 37% amino acid sequence identity to a functional bacterial rmlB, dTDP-Glc 4,6-dehydratase (25, 26), from *Salmonella*, *Streptococcus*, and 42% identity to the N-terminal portion of plant URS, Rhm ([supplemental Fig. S3A](#)) (18, 19). Such sequence identity was not sufficient to establish the function of the gene or determine whether the encoded protein utilizes dTDP-Glc or UDP-Glc. Thus, we cloned and expressed these genes in *E. coli* and then determined the enzymatic properties of the recombinant proteins.

Distinct protein bands (~52.5 and 52 kDa) were detected by SDS-PAGE of extracts from *E. coli* cells overexpressing recombinant UG4,6-Dh from *B. fuckeliana* and *M. grisea*, respectively (Fig. 3A, lanes 1 and 2), but were absent in *E. coli* cells express-

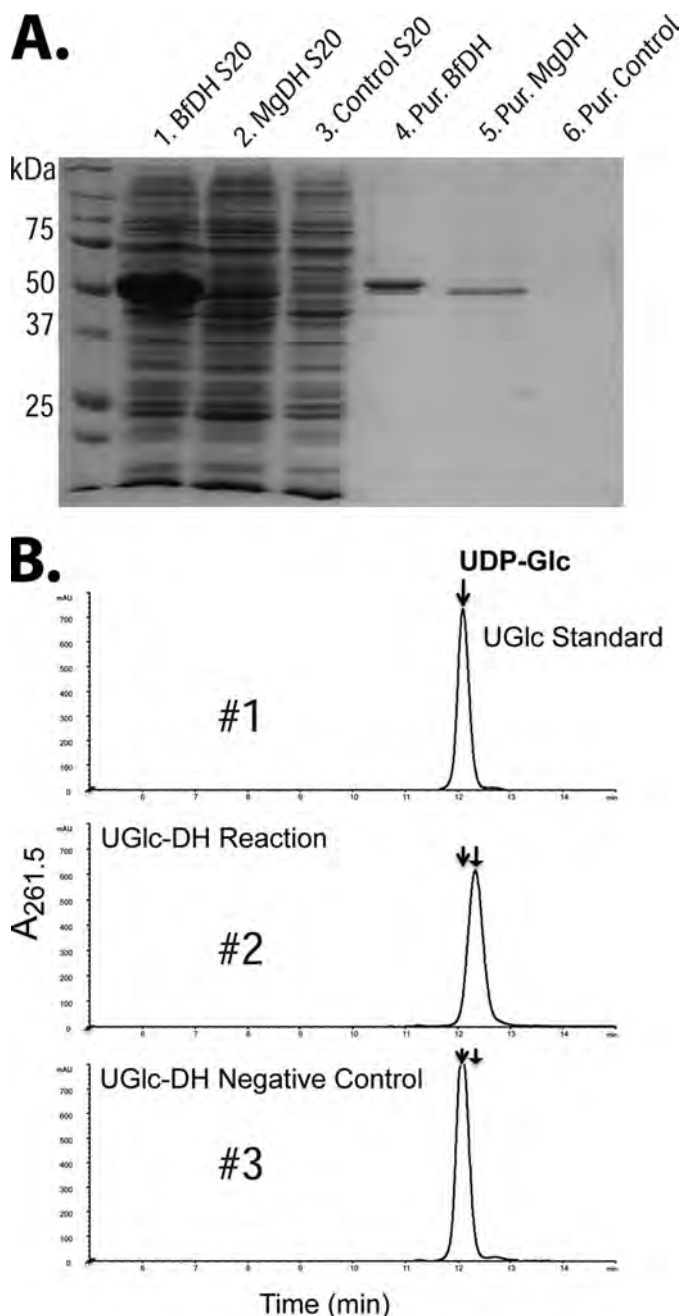


FIGURE 3. Expression and characterization of recombinant UDP-Glc-4,6-dehydratase. A, SDS-PAGE of total soluble protein isolated from *E. coli* cells expressing UG4,6-Dh from *B. fuckeliana* (lane 1), *M. grisea* (lane 2), control empty vector, and of the nickel column purified (Pur.) UG4,6-Dh (lanes 4 and 5), or empty vector control (lane 5). B, Mono Q high performance anion-exchange chromatography of the products formed by UG4,6-Dh. Purified recombinant UG4,6-Dh (panel #2) was reacted with UDP-Glc for 30 min in the presence of NAD^+ . The nickel column purified protein isolated from cells expressing the empty vector was reacted with UDP-Glc and NAD^+ for 45 min (panel #3) as a control. The distinct UDP-sugar peak marked by right-most arrow (with a retention time of 12.3) was collected and characterized by 1H NMR spectroscopy. The activity of total protein isolated from cells expressing recombinant UG4,6-Dh (panel #2) or vector control (panel #3) is shown.

ing the empty vector. The expressed UG4,6-Dh proteins were purified (Fig. 3A, lanes 4 and 5) and shown, using a HPLC-based assay, to convert UDP-Glc in the presence of NAD^+ to a new UDP-sugar. The newly formed UDP-sugar eluted from the ion-exchange column with a retention time of 12.3 min, although its

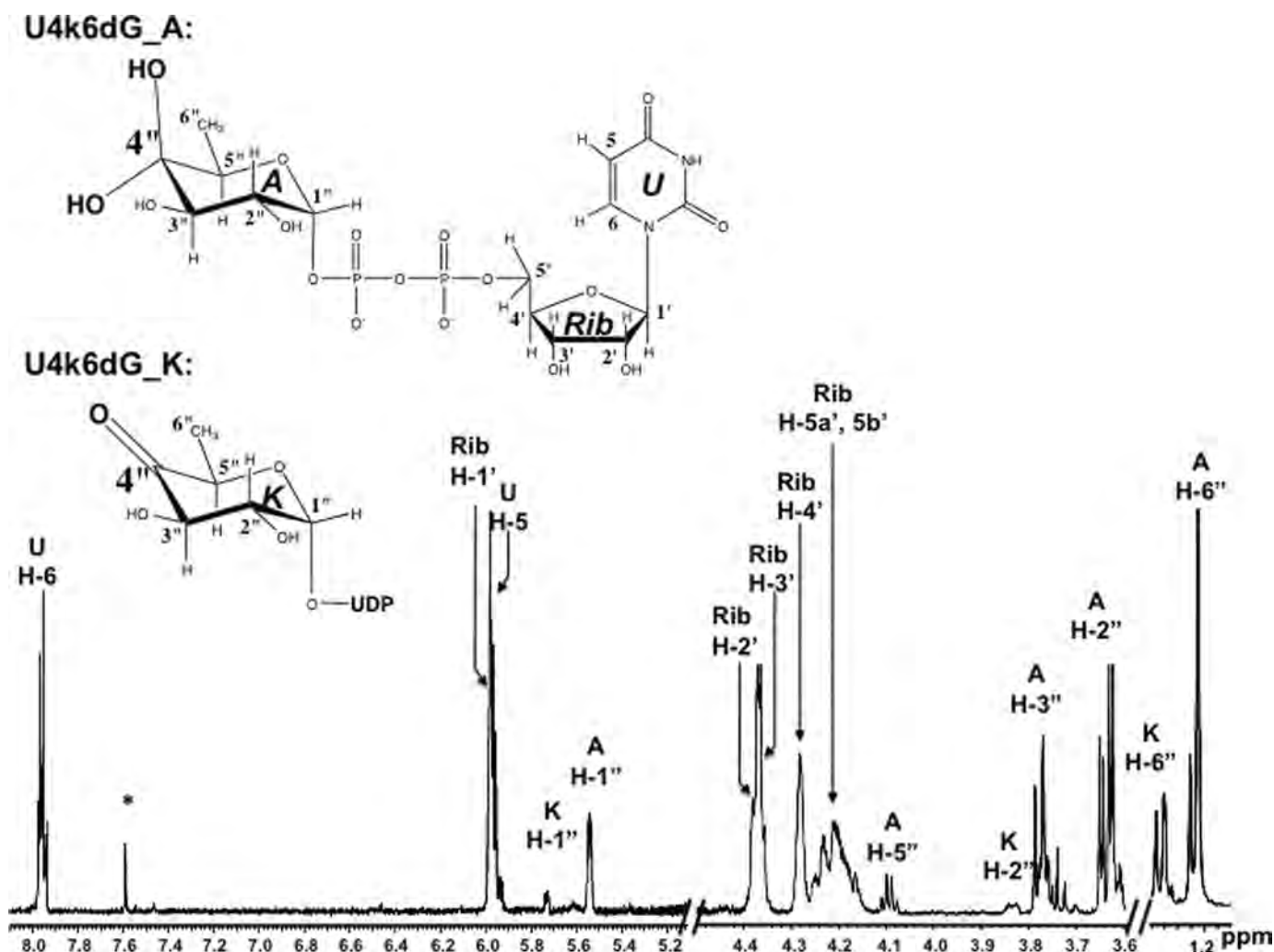


FIGURE 4. ^1H NMR spectroscopic analyses of UDP-Glc-4,6-dehydratase (UG4,6-Dh) reaction product indicate formation of two UDP-4-keto-6-deoxyglucose molecular species. The peak (Fig. 3B, panel #2, marked by right-most arrow) corresponding to the product formed by UG4,6-Dh was collected and analyzed by ^1H NMR spectroscopy at 600 MHz. A portion of the one-dimensional NMR spectrum between 1.18 and 1.30, 2.5 and 4.5, and 4.9 and 8.1 ppm is shown. H denotes signals for uracil (Ura) protons, H' are ribose (Rib) protons, and H'' are protons from 4-keto-6-deoxyglucose (U4k6dG_A hydrated and U4k6dG_K keto form). Note the diagnostic $H-1''$ (anomeric) and $H-6''$ signals for both major and minor products. * indicates HPLC column impurities.

substrate UDP-Glc eluted at 12.2 min (Fig. 3B, panel #2, marked by right arrow). Somewhat unexpectedly, the negative ion ESI mass spectrum of this material contained two ions, a major ion at m/z 565.04 and a less prominent ion at 547.06 (supplemental Fig. S4A). The ion at m/z 547.06 likely corresponds to UDP-4-keto-deoxyhexose (supplemental Fig. S4B). MS-MS analysis of the ion at m/z 565.04 gave an ion at m/z 323.77 (supplemental Fig. S4C), consistent with UMP, and suggested that this component was also a UDP-sugar. The masses of the two ions differed by 18 mass units suggesting a difference in hydration. However, the structure of the component corresponding to the ion at m/z 565.04 could not be determined from the MS data alone. Thus, the material eluting at 12.3 min was characterized by NMR spectroscopy (Fig. 4 and supplemental Table S2).

One-dimensional proton NMR analysis indicated that the enzymatic product UDP-4-keto-6-deoxyglucose exists in two forms (Fig. 4). The predominant component is the hydrated form and a minor component the keto form. The anomeric region of the ^1H spectrum contains two quadruplet signals with

chemical shifts of δ 5.73 ppm for the keto and δ 5.54 ppm for the hydrated form (Fig. 4). The distinct chemical shifts (supplemental Table S2) of $H1''$ and the coupling constant values of 3.7 Hz for $J_{H1'', H2''}$ and 7.0 Hz for $J_{H1'', P}$ are consistent with an α -linkage to the phosphate of UDP. The chemical shifts for the $H6''$ (1.265 and 1.215 ppm for keto and hydrate, respectively), and $H5''$ of the hydrate (4.09 ppm) are consistent with UDP-4-keto-6-deoxyglucose (19). The ^1H NMR spectrum obtained at 45 $^\circ\text{C}$ showed the $H5''$ signal (4.74 ppm) of the keto form that is hidden by the water peak at lower temperatures. Correlations in a two-dimensional TOCSY spectrum confirmed the assignments of $H2''$, $H3''$, and $H5''$ in both species. Like $H5''$, $H3''$ adjacent to the 4-keto carbon is shifted downfield to 4.64 ppm. The $J_{H2'', H3''}$ large coupling constant of 10.2 Hz is consistent with retention of the α -gluco-configuration. As expected, no proton signal was observed for $C4'$; thus ^{13}C NMR was used to confirm the presence of a 4-deoxy carbon. An HSQC experiment with UDP- ^{13}C 4k6dG confirmed the results from the proton data (see supplemental Table S2), and an HMBC experiment gave a cross-peak at 95 ppm between the 6-deoxy protons (here split

UDP-rhamnose Formation in Fungi

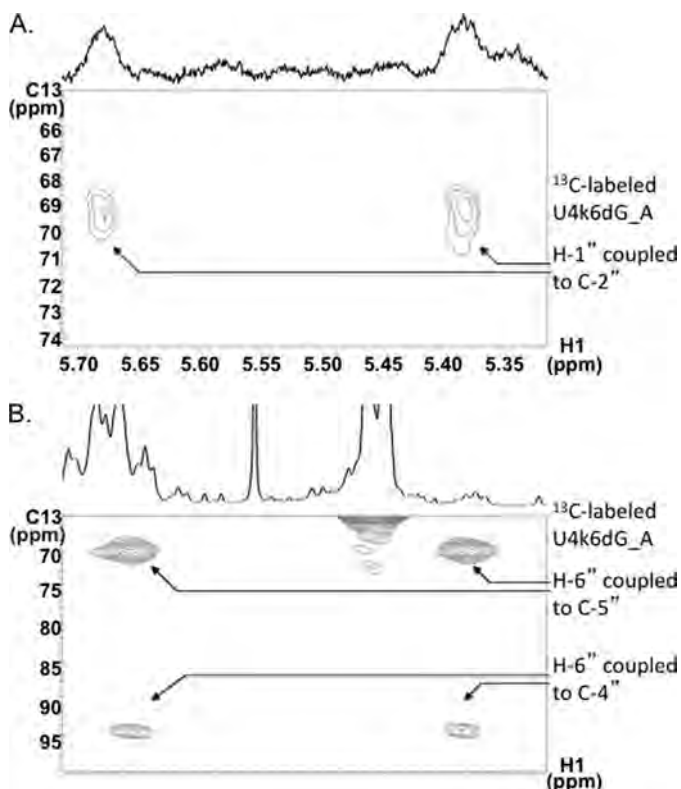


FIGURE 5. HMBC analysis confirms ^{13}C -labeled UDP-4-keto-6-deoxyglucose in hydrate form. UDP- ^{13}C Glc was reacted with UDP-Glc 4,6-dehydratase, and the product was analyzed by two-dimensional HMBC NMR. *A*, anomeric H-1'' of the major product U4k6dG_A (hydrate) is coupled to ^{13}C -2''. *B*, H-6'' of the hydrate product is coupled to ^{13}C -5'' and ^{13}C -4''. No signal was observed for the minor product, U4k6dG_K, as concentration was too low. The corresponding one-dimensional ^1H spectrum is displayed above each magnified region.

by $J_{\text{C}_6,\text{H}_6''}$) and C4 of the hydrated form (Fig. 5*B*). The expected cross-peak between H6'' and the 4-carbonyl of the keto form was not observed in this spectrum possibly due to its low concentration. The formation of two U4k6dG molecular ions (hydrated and keto) is also observed when real time NMR-based enzymatic reactions were carried out (see H1'' anomeric region Fig. 6, *A*, and H6'' protons region in *B*).

Our NMR data provide an explanation for the presence of the two molecular ions observed by ESI-MS. The major ion at m/z 565.04 originates from the hydrated species of U4k6dG and the minor ion at m/z 547.06 originates from the keto form of U4k6dG. Collectively, our data provides compelling evidence that the fungal gene encodes a protein with 4,6-dehydratase activity that converts UDP-Glc to UDP-4-keto-6-deoxyglucose (U4k6dG).

We then used time-resolved ^1H NMR to determine whether the UG4,6-Dh also converts dTDP-Glc to its 4-keto form (supplemental Fig. S5, *A* and *B*). However, this enzymatic reaction is much less efficient than the conversion of UDP-Glc to U4k6dG (compare Fig. 6*A* and supplemental Fig. S5*A*). Two dTDP-4k6dG molecular species were also observed in solution with chemical shifts for the H6'' 1.216 and 1.258 ppm (supplemental Fig. S5*B*) for keto and hydrate, respectively. H5'' of the hydrate (4.09 ppm) is consistent with dTDP-4-keto-6-deoxyglucose. Two forms of dTDP-4-keto-6-deoxyglucose have also been reported to exist in solution (14).

We identified several UG4,6-Dh homologs when we compared the *M. grisea* protein sequence with EST databases of transcribed fungal genes or with predicted ORFs from fungal genomes (see supplemental Fig. S3*A*). However, no comparable genes were identified in *Saccharomyces cerevisiae*, *Schizosaccharomyces*, and *Cryptococcus neoformans* indicating that not all fungi form UDP-4-keto-6-deoxyglucose. Phylogenetic analysis (supplemental Fig. S3*B*) suggests that fungal UG4,6-Dh encoding genes are clustered in a distinct clade and are separated from other eukaryotic homologs. Moreover, fungi that affect plants and humans have UG4,6-Dh genes that cluster in separate clades.

Protein sequence alignment (supplemental Fig. S3*A*) showed conserved regions between the fungal UDP-Glc 4,6-Dh proteins, a plant UDP-Glc 4,6-Dh protein (22, 23), and bacterial dTDP-Glc 4,6-Dh (rmlB) whose structure is known (16, 27). The bacterial proteins belong to the short chain dehydrogenase/reductase family, and contain the tyrosine-dependent oxidoreductase sequence $^{230}\text{YXXXX}^{234}$ (Tyr 167 in *Salmonella*). This sequence is believed to facilitate abstraction of the H4'' hydride to NAD^+ and, in concert with $^{194}\text{TDE}^{196}$, promote the oxidation of C-4'', the elimination of water, and the transfer of the hydride from NADH to C-6'' (boldface in supplemental Fig. S3*A*). Some of these amino acid sequences are also present in other UDP-sugar 4-epimerases and UDP-xylose synthase (28). The conserved $^{51}\text{GXXGXX}(\text{G}/\text{A})$ is likely involved in the cofactor-binding site. In some of the enzymes, including UDP-xylose synthase, the NAD^+ is tightly bound. By contrast, the fungal UG4,6-Dh loses the cofactor during chromatography and does not react with UDP-Glc unless NAD^+ is added (data not shown).

U4k6dG-ER Encodes a Bi-functional U4k6dG 3,5-Epimerase and 4-Reductase; Identification of Gene Involved in UDP-rhamnose Synthesis—BLAST searches using bacterial rmlC, rmlD (ADR74245, ADO64235, and BAS1139), and plant NRS/ER (At1g61300) identified fungal homologs (see supplemental Fig. S6*A*) of these proteins. The *M. grisea* protein shares 28 and 57% amino acid sequence identity to the bacterial 3,5-epimerase (rmlC) (15) and the plant NRS/ER (19), respectively.

The *M. grisea* and *B. fuckeliana* homologs were cloned, expressed, and their specific activities determined. A 36.8- and a 36.7-kDa protein was purified from *E. coli* strains overexpressing the recombinant protein from *M. grisea* and *B. fuckeliana*, respectively (Fig. 7*A*). No new products were detected when the *M. grisea* protein was reacted with U4k6dG alone (data not shown). However, when the reaction contained U4k6dG and NADPH , two new products were identified by HPLC (Fig. 7*B*, panel #2). The first peak at 11.5 min had a maximum UV absorbance at 259 nm and a retention time identical to NADP^+ . The ESI mass spectrum of the second peak (12.2 min) contained a major ion at m/z 549.04 (supplemental Fig. S7*A*). Collision-induced fragmentation gave an ion at m/z 323.47 (supplemental Fig. S7*B*) indicative of UMP. Together, these data are consistent with the formation of a UDP-deoxyhexose.

NMR spectroscopic analysis of the enzymatic product (Fig. 8 and supplemental Table S3) showed the presence of an anomeric proton with a chemical shift at δ 5.21 ppm and coupling

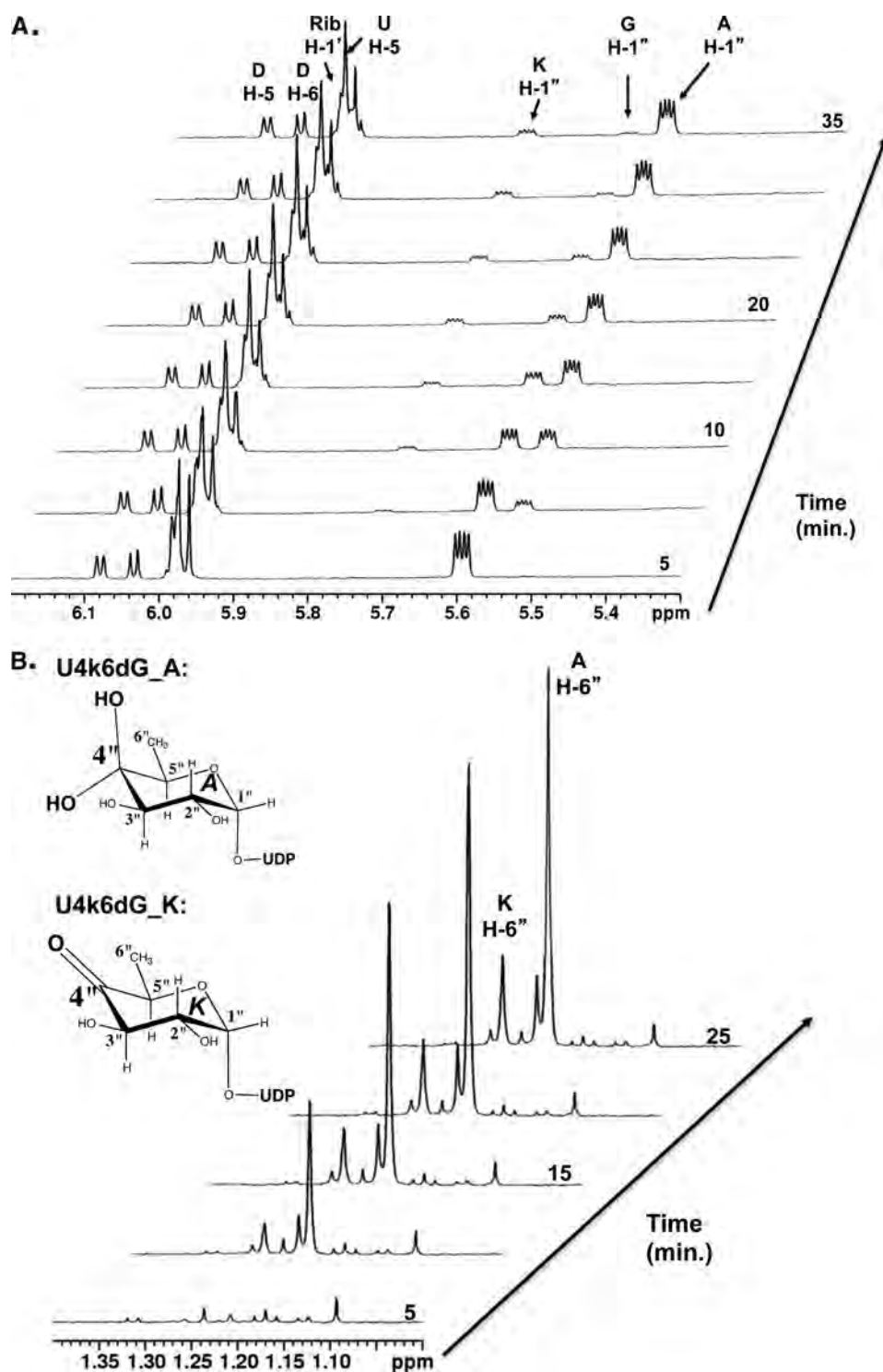


FIGURE 6. Real time ¹H NMR of UDP-Glc,4,6-dehydratase (UG4,6-Dh) reaction. The reaction was carried out at 30 °C for 35 min. The selected region for the diagnostic anomeric protons of reactant and product is shown between 5.3 and 6.2 ppm (A), and the diagnostic H-6'' of both forms of U4k6dG (A, hydrated; and K, keto) is shown between 0.9 and 1.4 ppm (B). Note the higher ratio of the hydrated to the keto form is consistent in both anomeric and H6'' regions. Fewer time-resolved spectra are displayed to prevent overcrowding peaks in B, and the reaction trends continue over the course of the reaction.

smaller than 2 for $J_{H1'',H2''}$ and 8.8 Hz for $J_{H1'',P}$. This small coupling (<2) explains the apparent doublet anomeric signal rather than a quadruplet signal. Two-dimensional HMBC analysis of ¹³C-labeled UDP- β -L-rhamnose shows that the anomeric H-1'' of UDP-Rha is coupled to ¹³C-2'' and that the H-6'' of UDP-Rha is coupled to ¹³C-5 (supplemental Fig. S8, A and B).

The chemical shifts and couplings of these signals are indicative of ¹³C-labeled rhamnose (1,6-deoxymannose). To confirm a β -linkage in UDP-Rha, a ¹³C HSQC NMR observation was carried over to determine the coupling between C1'' and H1''.

Consistent with a β -linkage was the C-1 chemical shift of δ 95.51 and $J_{C1'',H1''}$ coupling of 161 Hz. The small chemical

UDP-rhamnose Formation in Fungi

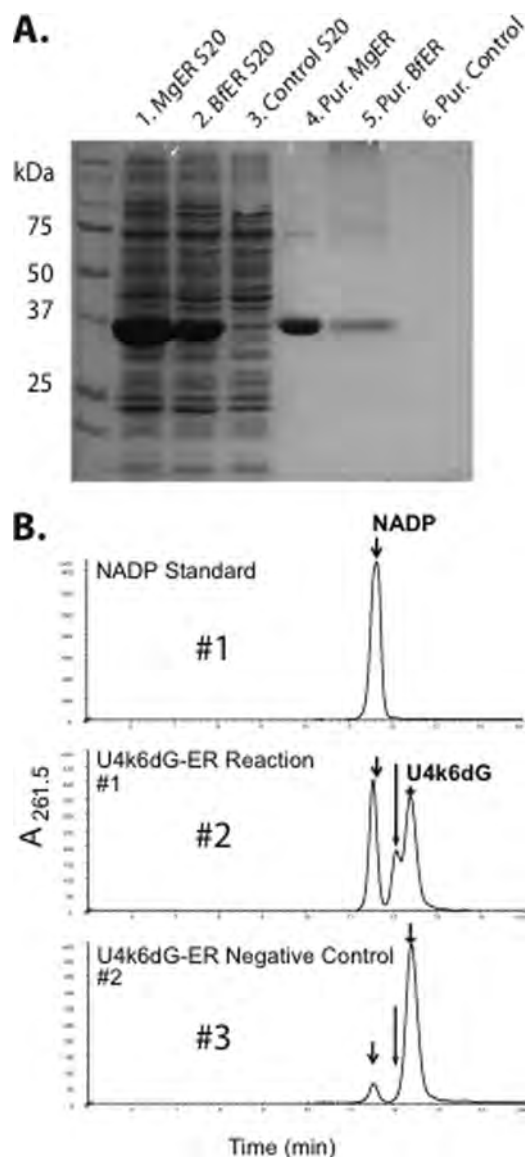


FIGURE 7. Expression and characterization of UDP-4-keto-6-deoxyglucose-3,5-epimerase/-4-reductase (U4k6dG-ER). A, SDS-PAGE of total soluble protein isolated from *E. coli* cells expressing U4k6dG-ER from *B. fuckeliana* (lane 1), *M. grisea* (lane 2), control empty vector, and of nickel column purified U4k6dG-ER (lanes 4 and 5), or empty vector control (lane 6). B, HPLC analysis of the products formed by U4k6dG-ER reacting with UDP-4-keto-6-deoxyglucose (U4k6dG). U4k6dG-ER was reacted with U4k6dG for 30 min in the presence of NADPH (panel #2). The purified protein isolated from cells expressing control empty vector was incubated with U4k6dG, and NADPH for 45 min (panel #3) is a control. The distinct UDP-sugar peak marked by the longest arrow (panels 2 and 3 with the same retention time 12.1) was collected and analyzed by ^1H NMR spectroscopy and ESI-MS spectrometer.

shifts and coupling (3.4) between H-2'' and H-3'' is also indicative of Rha (*i.e.* *manno* configuration) when compared with the large coupling (10.2) of the 6-deoxygluco H-2'' and H-3'' (supplemental Tables S2 and S3).

Real Time NMR Assays of UG4,6Dh and U4k6dG-ER Activity— The enzymatic progression of the dehydratase and the epimerase/reductase was examined to determine whether other products were formed. To this end selected regions (H-1'' and H-6'') of the ^1H NMR spectra were analyzed (Fig. 6, A and B). The characteristic NMR signal having a quadruplet peak signal that corresponds to the anomeric proton of UDP-Glc (G)

(labeled G H-1'' at 5.58 ppm in Fig. 6A decreased, with the concomitant increase in a quadruplet signal corresponding to A H-1'' of UDP-4-keto-6-deoxyglucose hydrated from U4k6dG_A). The anomeric proton of the keto form of U4k6dG_K H-1'' (5.73 ppm) is also increased during the time course of the UG4,6-Dh reaction. No change was observed for the signals from NAD $^+$ (N) protons (supplemental Fig. S9A). Clear differences in the chemical shifts for the proton attached to C-6 of glucose were observed during the formation of U4k6dG_A and U4k6dG_K from UDP-Glc (Fig. 6B, marked by A H-6'' and K H-6'', respectively).

The real time ^1H NMR spectra of the products formed by the bifunctional enzyme (see Fig. 9) revealed that the H-1'' signals of U4k6dG (A and K) decreased with a concomitant increase in the Rha H-1'' signal of UDP-Rha. The appearance of signals with chemical shifts corresponding to H-5'' (3.43 ppm) and H-4'' (3.35 ppm) and the diagnostic C-6 methyl group of the rhamnosyl moiety provide additional evidence for the formation of UDP-Rha. In addition, the real time ^1H NMR established that NADPH is converted to NADP $^+$ during the C-4'' reduction (supplemental Fig. S9).

Collectively, the real time NMR-based enzyme assay provides compelling evidence for the transformation of UDP-Glc to UDP-Rha via a UDP-4-keto-6-deoxyglucose intermediate. We next have tried to address if the 3,5-epimerization reaction occurs independently of the 4-reduction. The U4k6dG-ER was incubated with UDP-4-keto-6-deoxyglucose in the absence of NADPH, and the reaction was followed by NMR. However, no distinct chemical shift belonging to proton 2'' or 3'' was observed to indicate 3,5-epimerization. But when NADPH was added, UDP-Rha was formed as well as NADP $^+$. This suggests that the epimerization occurs, although the intermediate (UDP-4-keto-rhamnose) is bound to the enzyme and not released.

Enzymatic Properties of Dh and ER—UG4,6-Dh had maximum activity between 25 and 30 °C and was active across a wide pH range, with maximal activity at neutral pH (supplemental Fig. S10, A and B). Similar pH and temperature enzymatic activity profiles were observed with U4k6dG-ER (supplemental Fig. S11, A and B). The UG4,6-Dh activity was eluted from size-exclusion column with mass of 140,000 suggesting the fungal enzyme is active predominantly as a dimer-trimer (supplemental Fig. S12). Our recombinant UG4,6-Dh preparation included for long term storage stability the addition of 10 μM NAD $^+$. The fungal U4k6dG-ER, however, eluted from Superdex75 size-exclusion column at the void volume but was enzymatically inactive. Chromatography with different buffers failed to elute active U4k6dG-ER. Hence, the elution of U4k6dG-ER as a large mass may not reflect the size of active U4k6dG-ER in solution. It is possible that U4k6dG-ER aggregates on the gel, explaining, in part, no activity.

UG4,6-Dh requires NAD $^+$ for complete conversion of UDP-Glc to product. U4k6dG-ER requires NADPH for the reduction of U4k6dG to UDP-Rha. NADP $^+$ did not substitute NAD $^+$ for the dehydrogenation reaction nor did NADH substitute for NADPH for the reduction reaction. The latter result confirms earlier reports with plant NRS/ER (19) and viral U4k6dG-ER (29) and suggests a strict recognition of the U4k6dG-ER enzymes for the phosphoryl group O-C'2-linked to ribosyl group of the adenine moiety in NADPH. Substrate specificity of

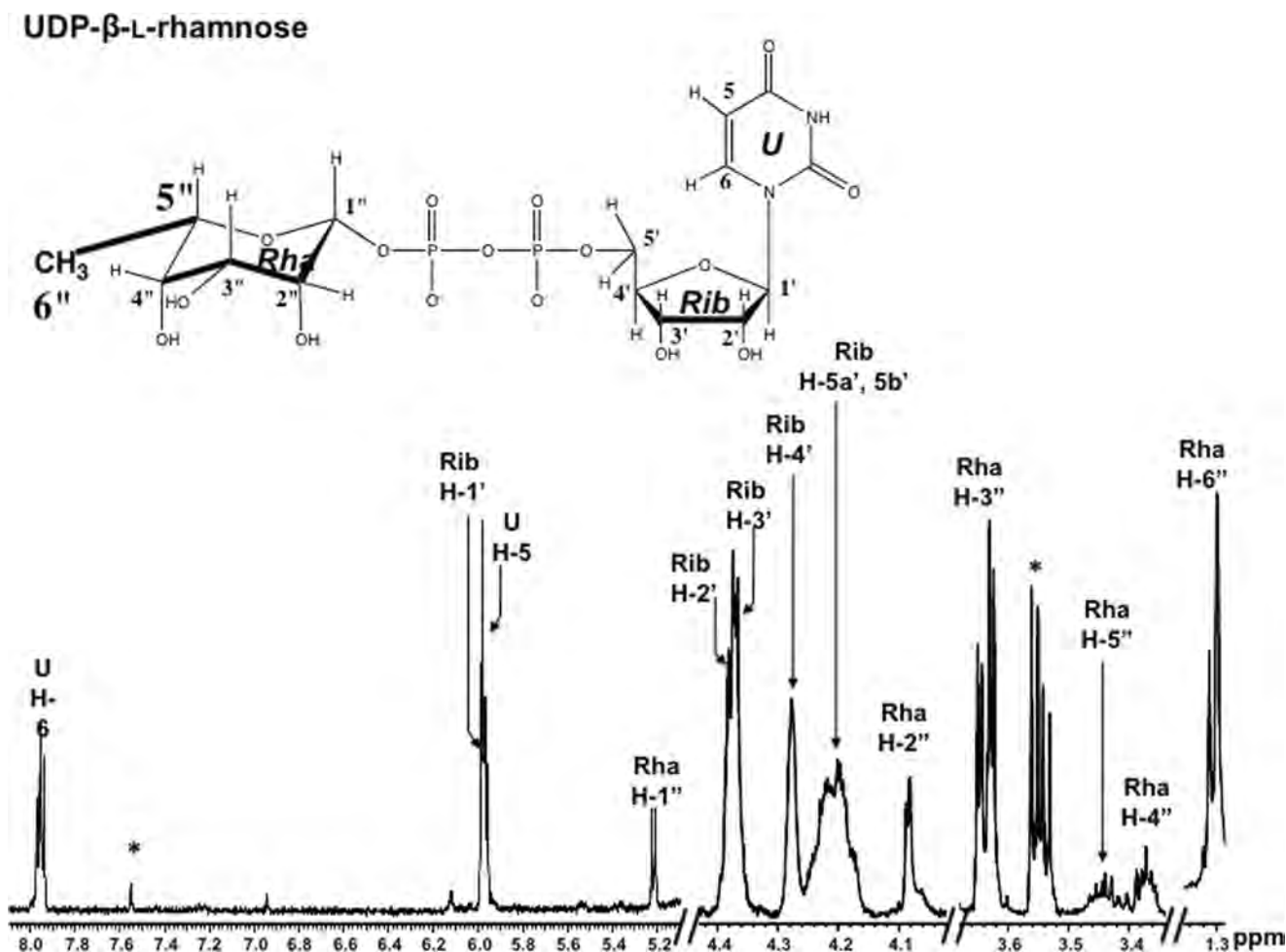


FIGURE 8. ^1H NMR spectroscopic analysis of UDP-4-keto-6-deoxyglucose-3,5-epimerase/-4-reductase (U4k6dG-ER) reaction product indicates formation of UDP- β -L-Rha. U4k6dG-ER reaction product was purified by HPLC and analyzed by ^1H NMR spectroscopy at 600-MHz at 25 °C. Portions of the NMR spectrum between 1.28 and 1.34, 3.3 and 3.7, 4.0 indicates ribose (Rib) protons, and H[*dprime*] indicates protons from rhamnose (Rha). Note the diagnostic H-1'' (anomeric) and H-6'' signals. * indicates HPLC column impurities.

UG4,6-Dh indicates that the fungal enzyme is unable to convert ADP-Glc, GDP-Glc, or UDP-GlcNAc to a product (data not shown). Although UG4,6-DH is able to convert dTDP-Glc to the corresponding dTDP-4-keto-6-deoxyglucose keto and hydrate forms, the catalytic efficiency (k_{cat}/K_m) is $0.0027 \mu\text{M s}^{-1}$, ~ 400 times lower than that for UDP-Glc. Inhibition studies determine that UDP and to a lesser degree UTP are inhibitors of UG4,6-Dh. The UG4,6-Dh was not inhibited however by NADH. UTP had a similar adverse activity with U4k6dG-ER (supplemental Tables S5 and S6). Kinetic analyses of UG4,6-Dh and U4k6dG-ER are shown in supplemental Table S7, A and B.

Further synergistic reactions containing both enzymes, NAD⁺ and NADPH showed that UG4,6-DH is strongly inhibited, whereas U4k6dG-ER is minimally inhibited, possibly because of NAD⁺. The inhibition of UG4,6-DH was likely due to UDP-Rha because in separate experiments 80% of UG4,6-DH activity was inhibited in the presence of 1 mM UDP-Rha (supplemental Table S5).

Transcripts and Glycosyl Analyses—The transcripts encoding UG4,6-Dh and U4k6dG-ER were detected in *M. grisea* spores but not in 10-day-old mycelium (Fig. 10A, compare lanes 4 and 5 and 9 and 10). Glycan isolated from *M. grisea* (Fig.

10B) shows that spores consisted of Rha, Gal, and Man residues, but mycelium and the EPS fractions consisted of Man and Gal; and no Rha residue was found. Unlike *M. grisea*, the UDP-Rha biosynthetic genes of *B. fuckeliana* were expressed in both spores and mycelium (Fig. 10C, lanes 11–14). Rha-containing glycans were also detected in these tissues as well as in an extracellular glycan fraction, EPS (Fig. 10D).

DISCUSSION

Our study is the first to provide evidence for the existence of UDP-Rha in fungi and the identification of two enzymes required to form this activated sugar from UDP-Glc in *M. grisea* and *B. fuckeliana*.

We have shown that both *M. grisea* and *B. fuckeliana* synthesize rhamnose-containing glycans. Preliminary data³ suggest that rhamnose-containing glycans are secreted 2 h after *M. grisea* spores germinate on artificial substrates. This glycan may protect the spore from desiccation and facilitate adherence to host, as has been suggested for the germination of *Colletotrichum graminicola* conidia (6, 13). Interestingly, the rhamnose-

³ J. Smith and M. Bar-Peled, unpublished data.

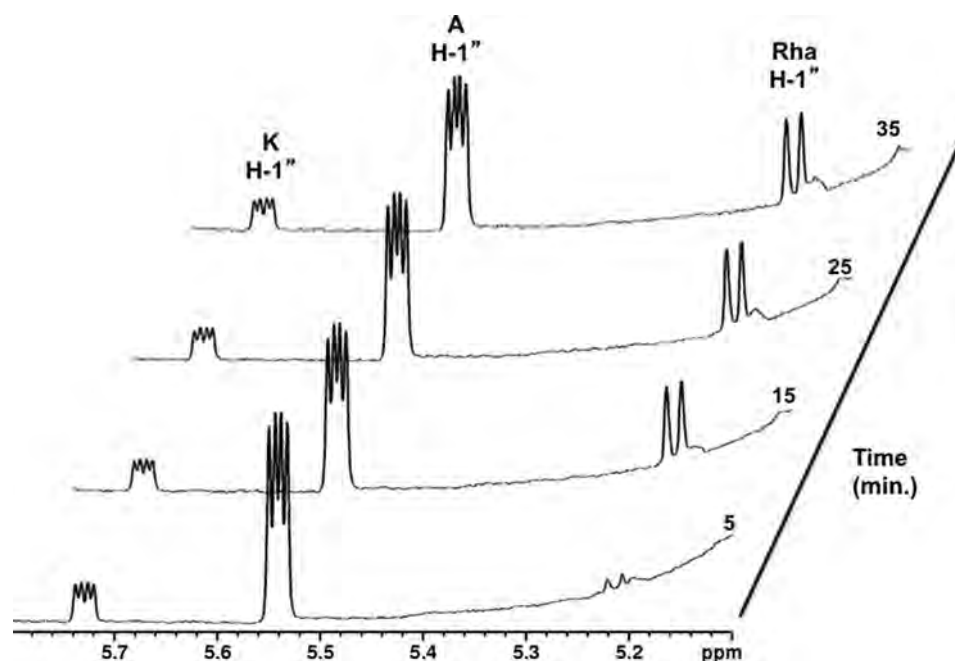


FIGURE 9. Real time ^1H NMR analysis of UDP-4-keto-6-deoxyglucose-3,5-epimerase/-4-reductase (*U4k6dG-ER*) reaction. The reaction was carried out at 30°C for 35 min. The selected region for the diagnostic anomeric protons of reactant and product is shown between 5.1 and 5.8 ppm. Note the appearance of a diagnostic quadruplet signal is a "doublet" due to very small coupling constant between phosphate and H1".

containing glycans accumulate differentially in *M. grisea*. Similarly, the genes encoding enzymes involved in UDP-Rha are also expressed in a tissue-specific manner.

Unlike *M. grisea*, the UDP-Rha biosynthetic genes of *B. fuckeliana* are expressed in both spores and mycelium. Likewise, Rha-containing glycans were also detected in these tissues as well as in an extracellular fraction. The ratio of Rha-containing glycans varies among the fungal tissues, and further detailed structural analyses will be required. Nonetheless, the display of Rha-containing glycans correlates with the expression of the genes for the synthesis of UDP-Rha. This suggests that the formation of UDP-Rha and the synthesis of Rha-containing glycans in fungi could be regulated in a tissue-specific manner. What molecular mechanism is involved in such expression is currently under investigation.

Analysis of the literature describing rhamnose-containing glycans in other fungal species indicates that these glycans are also accumulated in a tissue-specific manner or in response to growth conditions. For example, the extracellular aspartic proteinase from the zygomycete fungus *Phycomyces blakesleeanus* is a glycoprotein that contains mannose and rhamnose (30). Secretion of this glycoprotein occurs only at later stages of growth and can be modified by the nutrient composition of the culture media. In contrast, a Rha-containing glycoprotein was reported to be secreted only when *C. graminicola* spores attach to the host surface (13). There is also evidence that different types of rhamnose-containing polysaccharides accumulate during development of *Hericium erinaceus* fruiting bodies (31). One of the *Hericium* polysaccharides contains Rha linked to a fucogalactan (31), in a second the Rha is 3-*O*-methylated, and in a third, Rha exists in a rhamnoglucogalactan (32). Rhamnose has also been detected in the mature fruiting body of the black Perigord truffle (*Tuber melanosporum*) but not in other stages

of fungal growth (33). Taken together, synthesis of rhamnose-containing glycans (glycoproteins or polysaccharides) in fungi appears to be regulated.

Some fungi that infect humans also have rhamnose-containing glycans. For example, *Sporothrix schenckii*, the etiological agent of subcutaneous mycosis disease, secretes a glycoprotein that is heavily glycosylated. The *N*-linked glycan portion of this glycoprotein is composed of mannose and rhamnose and is believed to be involved in the adherence of the fungus to dermal tissue (34). The opportunistic human pathogen *Candida albicans*, the causal agent of candidiasis, when grown under conditions that favor biofilm production secretes a large exopolysaccharide composed of rhamnose, mannose, glucose, and glucosamine (35). However, under normal growth conditions, the yeast and hyphal forms lack rhamnose. In the human pathogen *Fonsecaea pedrosoi* (36), the appearance of rhamnose-containing glycans is also under tissue-specific regulation as rhamnose is predominant in conidia, whereas galactose is predominant in mycelia.

Based on genomic DNA sequence data, fungal species that have Rha-containing glycans also carry genes involved in UDP-4-keto-6-deoxyglucose and UDP-rhamnose synthesis. For example, *S. schenckii*, *Candida*, *C. graminicola*, and *T. melanosporum* have genes with homology to the *M. grisea* and *B. fuckeliana* genes identified in this report (as shown in [supplemental Figs. S3B and S6B](#)). Interestingly, the UDP-rhamnose biosynthetic genes of plant fungi are closer by phylogeny analysis to the plant species, when compared with the animal fungal biosynthetic genes. Of note is the clustering of the two viral UGlc4,6-Dh proteins (29). The chlorella virus co-living with plant appears to cluster with UGlc4,6-Dh in plants, although the same protein from the giant DNA virus that infects members of the genus *Acanthamoeba* is clustered with *Trypanosoma* ([supplemental Fig. S3B](#)). It would be of interest in the

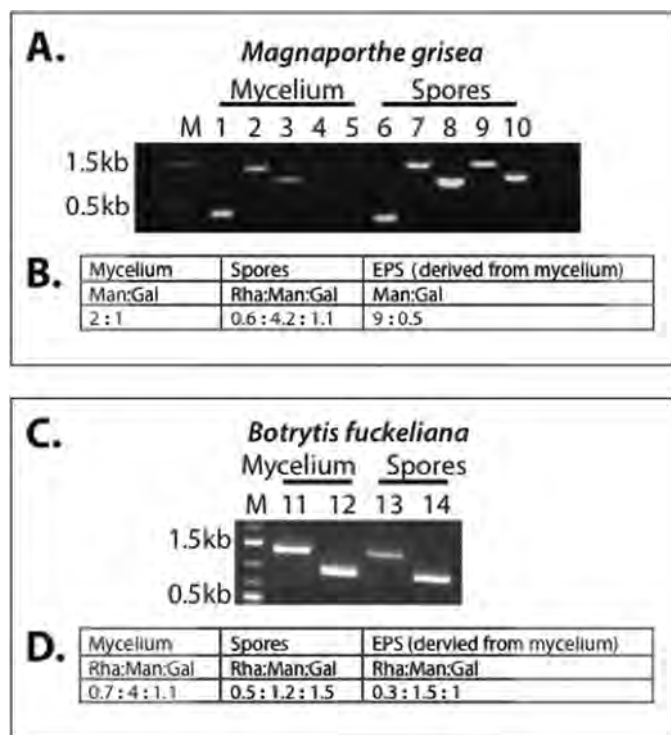


FIGURE 10. Glycosyl composition analysis and tissue-specific expression of genes involved in biosynthesis of UDP-rhamnose in *M. grisea* and *B. fuckeliana*. A, total RNA from *M. grisea* spores (lanes 1–5) and mycelium (lanes 6–10) was reverse-transcribed, and PCR was performed with primers specific for Mg_UG4,6-Dh (lanes 4 and 9) or Mg_U4k6dG-ER (lanes 5 and 10) or control, Ces1 (20) (lanes 1 and 2 and 6 and 7) and ARG2 (lanes 3 and 8). Note no apparent expression of UG4,6-Dh and U4k6dG-ER mRNA in *M. grisea* mycelium. B, glycosyl composition analyses of *M. grisea* spores, mycelia, and EPS derived from cultured mycelia grown for 10 days. The ratios of sugar residues were calculated from GC-MS. C, total RNA from *B. fuckeliana* spores (lanes 11 and 12) and mycelium (lanes 13 and 14) was reverse-transcribed and PCR with primers specific for Bf_UG4,6-Dh (lanes 11 and 13) or Bf_U4k6dG-ER (lanes 12 and 14). D, glycosyl composition analyses of *B. fuckeliana* spores, mycelia, and EPS derived from cultured mycelia grown for 10 days, the ratios of sugar residues were calculated from GC-MS.

future to look at many viral genomes and determine the role of UDP-Rha in these virus-host interactions.

As many as 200 fungi are known to impact human health (37). As far as we are aware, humans do not make Rha-containing glycans; thus, the metabolic pathways involved in the formation of rhamnose-containing glycans provide a potential target for drugs to control some fungal diseases in humans as well as other animals.

Additional research is required to structurally characterize the Rha-containing glycans synthesized by *M. grisea* and *B. fuckeliana*. Such information together with data obtained after reduction or elimination of these two UDP-Rha biosynthetic genes, will further illuminate the roles of rhamnose-containing glycans in fungi.

Acknowledgments—We thank Malcolm O'Neill of the Complex Carbohydrate Research Center for constructive comments on the manuscript. We also thank Dr. S.-C. Wu and Dr. C. Bergman of the Complex Carbohydrate Research Center for providing the fungal strains. NMR spectroscopy was performed at the SE Collaboratory for High Field Biomolecular NMR, a research resource at the University of Georgia, funded by National Institutes of Health Grant GM66340 from NIGMS and the Georgia Research Alliance.

REFERENCES

- Glazebrook, J. (2005) Contrasting mechanisms of defense against biotrophic and necrotrophic pathogens. *Annu. Rev. Phytopathol.* **43**, 205–227
- Valent, B., and Khang, C. H. (2010) Recent advances in rice blast effector research. *Curr. Opin. Plant Biol.* **13**, 434–441
- Zeigler, R. S., Leong, S. A., Teng, P. S., and C. A. B. International (1994) *Rice Blast Disease*, A CAB International Publication CABI Series, International Rice Research Institute, Wallingford, CT
- MacFarlane, H. H. (1968) *Review of Applied Mycology, Plant Host, Pathogen Index to Volumes 1–40*, pp. 1922–1969, Commonwealth Mycological Institute, UK
- Perfect, S. E., Hughes, H. B., O'Connell, R. J., and Green, J. R. (1999) Colletotrichum: A model genus for studies on pathology and fungal-plant interactions. *Fungal Genet. Biol.* **27**, 186–198
- Epstein, L., and Nicholson, R. L. (2006) in *Biological Adhesives* (Smith, A. M., and Callow, J. A., eds) pp. 41–62, Springer-Verlag, Berlin
- Hamer, J. E., Howard, R. J., Chumley, F. G., and Valent, B. (1988) A mechanism for surface attachment in spores of a plant pathogenic fungus. *Science* **239**, 288–290
- Pettolino, F., Sasaki, I., Turbic, A., Wilson, S. M., Bacic, A., Hrmova, M., and Fincher, G. B. (2009) Hyphal cell walls from the plant pathogen *Rhynchosporium secalis* contain (1,3/1,6)-beta-D-glucans, galacto-, and rhamnomannans, (1,3;1,4)-beta-D-glucans and chitin. *FEBS J.* **276**, 3698–3709
- Ahrzazem, O., Blazquez, G., Prieto, A., Bernabe, M., and Leal, J. A. (2002) Alkali-extractable and water soluble polysaccharide (F1 SS): A chemotaxonomic and phylogenetic character for *Cephalotheca*. *Mycol. Res.* **106**, 1187–1192
- Gorin, P. A., and Spencer, J. F. (1970) Structures of the L-rhamno-D-mannan from *Ceratocystis ulmi* and the gluco-D-mannan from *Ceratocystis brunnea*. *Carbohydr. Res.* **13**, 339–349
- Rizza, V., and Kornfeld, J. M. (1969) Components of conidial and hyphal walls of *Penicillium chrysogenum*. *J. Gen. Microbiol.* **58**, 307–315
- Molinario, A., Piscopo, V., Lanzetta, R., and Parrilli, M. (2002) Structural determination of the complex exopolysaccharide from the virulent strain of *Cryphonectria parasitica*. *Carbohydr. Res.* **337**, 1707–1713
- Ramadoss, C. S., Uhlig, J., Carlson, D. M., Butler, L. G., and Nicholson, R. L. (1985) Composition of the mucilaginous spore matrix of *Colletotrichum graminicola*, a pathogen of corn, sorghum, and other grasses. *J. Agric. Food Chem.* **33**, 728–732
- Thibodeaux, C. J., Melançon, C. E., and Liu, H. W. (2007) Unusual sugar biosynthesis and natural product glycodiversification. *Nature* **446**, 1008–1016
- Dong, C., Major, L. L., Srikannathasan, V., Errey, J. C., Giraud, M. F., Lam, J. S., Graninger, M., Messner, P., McNeil, M. R., Field, R. A., Whitfield, C., and Naismith, J. H. (2007) RmlC, a C3' and C5' carbohydrate epimerase, appears to operate via an intermediate with an unusual twist boat conformation. *J. Mol. Biol.* **365**, 146–159
- Hegeman, A. D., Gross, J. W., and Frey, P. A. (2002) Concerted and stepwise dehydration mechanisms observed in wild-type and mutated *Escherichia coli* dTDP-glucose 4,6-dehydratase. *Biochemistry* **41**, 2797–2804
- Ma, Y., Pan, F., and McNeil, M. (2002) Formation of dTDP-rhamnose is essential for growth of mycobacteria. *J. Bacteriol.* **184**, 3392–3395
- Oka, T., Nemoto, T., and Jigami, Y. (2007) Functional analysis of *Arabidopsis thaliana* RHM2/MUM4, a multidomain protein involved in UDP-D-glucose to UDP-L-rhamnose conversion. *J. Biol. Chem.* **282**, 5389–5403
- Watt, G., Leoff, C., Harper, A. D., and Bar-Peled, M. (2004) A bifunctional 3,5-epimerase/4-keto reductase for nucleotide-rhamnose synthesis in *Arabidopsis*. *Plant Physiol.* **134**, 1337–1346
- Wu, S. C., Ham, K. S., Darvill, A. G., and Albersheim, P. (1997) Deletion of two endo-β-1,4-xylanase genes reveals additional isozymes secreted by the rice blast fungus. *Mol. Plant-Microbe Interact.* **10**, 700–708
- Yang, T., Bar-Peled, L., Gebhart, L., Lee, S. G., and Bar-Peled, M. (2009) Identification of galacturonic acid-1-phosphate kinase, a new member of the GHMP kinase superfamily in plants, and comparison with galactose-1-phosphate kinase. *J. Biol. Chem.* **284**, 21526–21535
- Gu, X., Glushka, J., Lee, S. G., and Bar-Peled, M. (2010) Biosynthesis of a new UDP-sugar, UDP-2-acetamido-2-deoxyxylose, in the human patho-

- gen *Bacillus cereus* subspecies *cytotoxis* NVH 391-98. *J. Biol. Chem.* **285**, 24825–24833
23. York, W., Darvill, A., McNeil, M., Stevenson, T., and Albersheim, P. (1986) Isolation and characterization of plant cell wall components. *Methods Enzymol.* **118**, 3–40
 24. Turnock, D. C., and Ferguson, M. A. (2007) Sugar nucleotide pools of *Trypanosoma brucei*, *Trypanosoma cruzi*, and *Leishmania major*. *Eukaryot. Cell* **6**, 1450–1463
 25. Allard, S. T., Beis, K., Giraud, M. F., Hegeman, A. D., Gross, J. W., Wilmouth, R. C., Whitfield, C., Graninger, M., Messner, P., Allen, A. G., Maskell, D. J., and Naismith, J. H. (2002) Toward a structural understanding of the dehydratase mechanism. *Structure* **10**, 81–92
 26. Dong, S., McPherson, S. A., Wang, Y., Li, M., Wang, P., Turnbough, C. L., Jr., and Pritchard, D. G. (2010) Characterization of the enzymes encoded by the anthrose biosynthetic operon of *Bacillus anthracis*. *J. Bacteriol.* **192**, 5053–5062
 27. Allard, S. T., Giraud, M. F., Whitfield, C., Graninger, M., Messner, P., and Naismith, J. H. (2001) The crystal structure of dTDP-D-glucose 4,6-dehydratase (RmlB) from *Salmonella enterica* serovar Typhimurium, the second enzyme in the dTDP-L-rhamnose pathway. *J. Mol. Biol.* **307**, 283–295
 28. Williams, G. J., Breazeale, S. D., Raetz, C. R., and Naismith, J. H. (2005) Structure and function of both domains of ArnA, a dual function decarboxylase and a formyltransferase, involved in 4-amino-4-deoxy-L-arabinose biosynthesis. *J. Biol. Chem.* **280**, 23000–23008
 29. Parakkottil Chothi, M., Duncan, G. A., Armirotti, A., Abergel, C., Gurnon, J. R., Van Etten, J. L., Bernardi, C., Damonte, G., and Tonetti, M. (2010) Identification of an L-rhamnose synthetic pathway in two nucleocytoplasmic large DNA viruses. *J. Virol.* **84**, 8829–8838
 30. De Vicente, J. I., De Arriaga, D., Del Valle, P., Soler, J., and Eslava, A. P. (1996) Purification and characterization of an extracellular aspartate protease from *Phycomyces blakesleeana*. *Fungal Genet. Biol.* **20**, 115–124
 31. Zhang, A. Q., Zhang, J. S., Tang, Q. J., Jia, W., Yang, Y., Liu, Y. F., Fan, J. M., and Pan, Y. J. (2006) Structural elucidation of a novel fucogalactan that contains 3-O-methyl rhamnose isolated from the fruiting bodies of the fungus, *Hericium erinaceus*. *Carbohydr. Res.* **341**, 645–649
 32. Jia, L. M., Liu, L., Dong, Q., and Fang, J. N. (2004) Structural investigation of a novel rhamnoglucogalactan isolated from the fruiting bodies of the fungus *Hericium erinaceus*. *Carbohydr. Res.* **339**, 2667–2671
 33. Harki, E., Bouya, D., and Dargent, R. (2006) Maturation-associated alterations of the biochemical characteristics of the black truffle *Tuber melanosporum* Vitt. *Food Chem.* **99**, 394–400
 34. Ruiz-Baca, E., Toriello, C., Perez-Torres, A., Sabanero-Lopez, M., Villagomez-Castro, J. C., and Lopez-Romero, E. (2009) Isolation and some properties of a glycoprotein of 70-kDa (Gp70) from the cell wall of *Sporothrix schenckii* involved in fungal adherence to dermal extracellular matrix. *Med. Mycol.* **47**, 185–196
 35. Lal, P., Sharma, D., Pruthi, P., and Pruthi, V. (2010) Exopolysaccharide analysis of biofilm-forming *Candida albicans*. *J. Appl. Microbiol.* **109**, 128–136
 36. de A Soares, R. M., Angluster, J., de Souza, W., and Alviano, C. S. (1995) Carbohydrate and lipid components of hyphae and conidia of human pathogen *Fonsecaea pedrosoi*. *Mycopathologia* **132**, 71–77
 37. Taylor, L. H., Latham, S. M., and Woolhouse, M. E. (2001) Risk factors for human disease emergence. *Philos. Trans. R Soc. Lond. B Biol. Sci.* **356**, 983–989
 38. Beis, K., Allard, S. T., Hegeman, A. D., Murshudov, G., Philp, D., and Naismith, J. H. (2003) The structure of NADH in the enzyme dTDP-D-glucose dehydratase (RmlB). *J. Am. Chem. Soc.* **125**, 11872–11878